Implications of parity-violating electron scattering experiments on 48Ca (CREX) and 208Pb (PREX-II) for nuclear energy density functionals

Yüksel, Esra; Paar, Nils

Implications of parity-violating electron scattering experiments on ^{48}Ca (CREX) and ^{208}Pb (PREX-II) for nuclear energy density functionals

Esra Yüksel [a,*], Nils Paar [b]

[a] *Department of Physics, University of Surrey, Guildford, Surrey, GU2 7XH, United Kingdom*
[b] *Department of Physics, Faculty of Science, University of Zagreb, Bijenička c. 32, 10000 Zagreb, Croatia*

ABSTRACT

Recent precise parity-violating electron scattering experiments on ^{48}Ca (CREX) and ^{208}Pb (PREX-II) provide a new insight on the formation of neutron skin in nuclei. Within the energy density functional (EDF) framework, we investigate the implications of CREX and PREX-II data on nuclear matter symmetry energy and isovector properties of finite nuclei: neutron skin thickness and dipole polarizability. The weak-charge form factors from the CREX and PREX-II experiments are employed directly in constraining the relativistic density-dependent point coupling EDFs. The EDF established with the CREX data acquires considerably smaller values of the symmetry energy parameters, neutron skin thickness and dipole polarizability both for ^{48}Ca and ^{208}Pb, in comparison to the EDF obtained using the PREX-II data, and previously established EDFs. Presented analysis shows that CREX and PREX-II experiments could not provide consistent constraints for the isovector sector of the EDFs, and further theoretical and experimental studies are required.

© 2022 The Author(s). Published by Elsevier B.V. This is an open access article under the CC BY license (http://creativecommons.org/licenses/by/4.0/). Funded by SCOAP^3.

The nuclear equation of state (EOS) is essential for understanding the properties of strongly interacting many-body systems like atomic nuclei and neutron stars [1–3]. Constraining the density dependence of the nuclear symmetry energy, which is a key feature of the nuclear EOS, represents a long-standing and unresolved question in nuclear physics and astrophysics [3]. The fundamental source of this challenge is that the nuclear symmetry energy cannot be determined directly by experiment, thus it is necessary to identify and use relevant observables on finite nuclei to constrain their values [3]. The neutron skin thickness (ΔR_{np}) [4–8], dipole polarizability (α_D) [7,9–11], and neutron star mass-radius [12,13] have been established as key observables to constrain the isovector channel of the nuclear energy density functional (EDF) and the symmetry energy parameters of the nuclear EOS around the saturation density.

The recent precise parity-violating electron scattering experiments on ^{48}Ca (CREX) [14] and ^{208}Pb (PREX-II) [15] provide new insight into the neutron skin thickness in nuclei. Through the measurement of the parity violating asymmetry A_{PV}, these experiments allow to determine the nuclear weak-charge form factor F_W that is also strongly correlated with the density dependence

of the symmetry energy and the neutron skin thickness of nuclei, hence providing an important quantity to probe the isovector channel of the EDFs [16]. The weak charge form factor F_W is obtained with the Fourier transform of the weak charge density for a given momentum transfer. Since the charge density is known experimentally, the Coulomb distortions can also be corrected accurately. [17]. Therefore, the parity-violating electron scattering experiments provide precise and model-independent data with small uncertainties for the nuclear weak-charge form factor F_W, that could be used in constraining the EDFs [16,17]. The CREX [14] and PREX-II [15] experiments reported the weak-charge form factors of ^{48}Ca and ^{208}Pb as F_W(q=0.8733 fm^{-1})= 0.1304 ± 0.0052(stat)±0.0020(syst) and F_W(q=0.3978 fm^{-1})= 0.368± 0.013 (exp.), respectively. The measured parity violating asymmetry A_{PV} in ^{48}Ca and ^{208}Pb has recently been analyzed using EDFs, indicating that there are difficulties to describe A_{PV} simultaneously in both nuclei [18,19].

In this letter, we establish effective interactions based on the relativistic EDF with density-dependent point couplings, using recent nuclear weak-charge form factor F_W data from CREX [14] and PREX-II [15] experiments alongside with the selected ground state properties of nuclei. In this way, we aim to reveal the implications of the CREX and PREX-II experiments on the properties of finite nuclei and nuclear matter, especially the symmetry energy and its slope around the saturation density. By calculating the rel-

Table 1
The nuclear matter properties at saturation density for the DDPC-CREX, DDPC-PREX, and DDPC-REX interactions. The properties for the DD-PC1 [20] and DD-PCX [21] interactions are also given for comparison. The uncertainties of the obtained values are provided within the parenthesis.

	E/A (MeV)	m_D^*/m	K_0 (MeV)	J (MeV)	L (MeV)
DDPC-CREX	-15.989(16)	0.5672(5)	225.48(1.55)	27.01(23)	19.60(1.01)
DDPC-PREX	-16.108(19)	0.5680(7)	235.41(2.42)	36.18(0.80)	101.78(9.34)
DDPC-REX	-16.019(16)	0.5696(5)	242.95(76)	28.86(0.33)	30.03(2.06)
DD-PC1	-16.061	0.580	230.0	33.0	70.1
DD-PCX	-16.026(18)	0.5598(8)	213.03(3.54)	31.12(32)	46.32(1.68)

evant nuclear observables with the new interactions, in particular the neutron skin thickness and dipole polarizability, we discuss their relationship with the recent experimental data from parity violating electron scattering.

Theoretical framework employed in this study is based on the relativistic EDF, where the self-consistent solution of relativistic single-nucleon Kohn-Sham equations provides the nuclear ground state density and energy [22,23]. In the formulation given by the Lagrangian density, we use an effective interaction between nucleons described with four fermion contact interaction terms, including isoscalar-scalar, isoscalar-vector, isovector-vector and isospace-space channels [20,24]. It includes free nucleon terms, point coupling interaction terms, coupling of protons to the electromagnetic field, and the derivative term accounting for the leading effects of finite-range interactions. For a quantitative description of nuclear density distribution and radii, the derivative terms are also necessary [20]. The couplings in the interaction terms $\alpha_i(\rho)$ include explicit density dependence [24]. The point coupling model includes 10 parameters (a_S, b_S, c_S, d_S, a_V, b_V, d_V, b_{TV}, d_{TV} and δ_S) [24]. The relativistic Hartree-Bogoliubov (RHB) model [20,24,25] is used to describe open-shell nuclei, including the pairing field formulated using separable pairing force, which also contains two parameters for the proton and neutron pairing strengths (G_p and G_n) [26].

In this work, we employed the RHB model to constrain 12 model parameters by minimizing the χ^2 objective function with a set of observables on nuclear properties [21,24,27]. In order to benchmark the role of CREX and PREX-II data, in the χ^2 minimization we used the same nuclear ground state properties as in recent optimization of the DD-PCX interaction, i.e., the binding energies (34 nuclei), charge radii (26 nuclei), and mean pairing gaps (15 nuclei) (see supplementary material [28] for the details about selected nuclei and their properties). In the optimization of the new functionals we also used the latest nuclear weak-charge form factors F_W obtained from the CREX (^{48}Ca) [14] and PREX-II (^{208}Pb) [15] experiments. First we have established two functionals, DDPC-CREX and DDPC-PREX, optimized by using nuclear properties given above and the weak-charge form factor data of ^{48}Ca and ^{208}Pb, respectively. The adopted errors for F_W are taken as 0.5%, that is relatively tight in order to reproduce well the experimental F_W values. Next, an additional functional DDPC-REX is established, by employing weak-charge form factor data of both ^{48}Ca and ^{208}Pb, with the errors taken as 2.0%, to provide more flexibility to accommodate F_W data for the two nuclei. Following the optimization of the interactions, the statistical uncertainties of the model parameters are estimated using the co-variance analysis [29]. The parameters of these three new DDPC functionals and their uncertainties are given in supplementary material [28].

In Table 1, we present the nuclear matter properties: energy per nucleon E/A, effective mass (m_D^*/m), incompressibility K_0, symmetry energy J and slope of the symmetry energy L at saturation density [3], for new DD-PC functionals in comparison to the properties of the previously established DD-PC1 [20] and DD-PCX [21] interactions. We note that the symmetry energy parameters J and

L of the DDPC-CREX functional are considerably lower than those of the DDPC-PREX, while the DDPC-REX acquires intermediate values between the two former functionals. While the J and L values for the DDPC-CREX functional are lower than those of DD-PC1 and DD-PCX, the DDPC-PREX functional predicts much higher values. Our DDPC-PREX results are also consistent with the findings in Ref. [30], where J =38.1±4.7 MeV and L =106±37 MeV are obtained using the PREX-II data. The symmetry energy parameters for DDPC-CREX and DDPC-PREX interactions are outside rather broad ranges of their values obtained in the EDF analysis of dipole polarizability, $J = 30 - 35$ MeV and $L = 20 - 66$ MeV [11], and also at variance with the findings of previous studies (see Ref. [3] and the references therein.) Therefore, already at the level only of the nuclear matter properties, we observe considerable inconsistencies between the symmetry energy properties of new functionals constrained by weak-charge form factor data and previously established functionals that are known as successful in the description of a variety of nuclear properties, including DD-PCX [21] with carefully adjusted isovector channel using nuclear observables such as dipole polarizability.

The symmetry energy and its slope are known to be strongly correlated with the neutron skin thickness of nuclei [4–7]. However, accurate and model independent measurement of the neutron skin thickness of nuclei is rather challenging. The first Lead Radius EXperiment (PREX-I) [31] estimated very large neutron skin thickness for ^{208}Pb with significant uncertainties ($R_n - R_p = 0.33^{+0.16}_{-0.18}$). Recently, the new data from the PREX-II experiment has also been announced and the neutron-skin thickness of ^{208}Pb was found as $R_n - R_p$ =0.283±0.071 fm, obtained by combining the new data with the previous measurements [15]. The charge minus the weak form factor was also obtained as $F_{ch} - F_W = 0.041 \pm 0.013$ in the same experiment. Lately, CREX data has been announced and the neutron skin thickness and the form factor difference of ^{48}Ca have been obtained as $R_n - R_p$ =0.121±0.026(exp)±0.024(model) fm and $F_{ch} - F_W = 0.0277 \pm 0.0055$, respectively [14]. In the following, we discuss the isovector properties of nuclei calculated using our three point coupling interactions constrained by F_W, in comparison to those of previously established EDFs and experimental data.

Fig. 1 shows the neutron skin thickness $\triangle R_{np}$ for ^{48}Ca and ^{208}Pb as a function of the difference of charge and weak-charge form factors, $F_{ch} - F_W$, from calculations based on relativistic EDFs. The neutron skin thickness of a nucleus is calculated as $\triangle R_{np} = \langle r_n^2 \rangle^{1/2} - \langle r_p^2 \rangle^{1/2}$, and $\langle r_{n(p)}^2 \rangle^{1/2}$ represents neutron (proton) root-mean-square radii. The results of new point coupling functionals DDPC-CREX, DDPC-PREX, and DDPC-REX are compared with those of the DD-PC1 [20], DD-PCX [21], and family of eight DD-PC functionals that cover a range of the symmetry energy values at saturation density $J = 29, 30, ..., 36$ MeV [32], density dependent meson-exchange functionals DD-ME1 [33] and DD-ME2 [34], and the corresponding family of five DD-ME functionals with $J = 30, 32, ..., 38$ MeV. The neutron skin thickness is strongly correlated with the $F_{ch} - F_W$ values, both for ^{48}Ca and ^{208}Pb. For ^{48}Ca, only a few interactions are within the ranges of $F_{ch} - F_W$
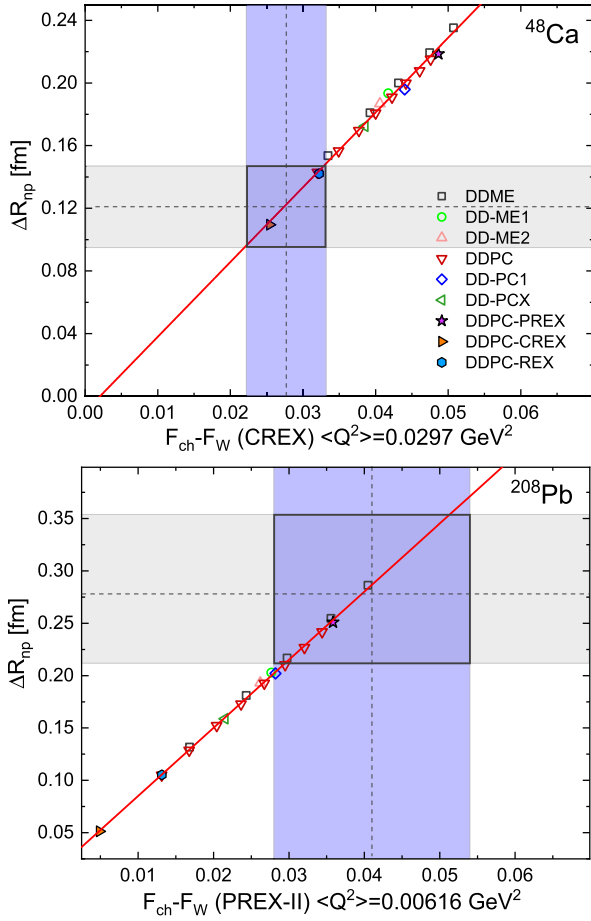
Fig. 1. The neutron skin thickness ΔR_{np} of ^{48}Ca (upper panel) and ^{208}Pb (lower panel) as a function of the form factor difference $F_{ch} - F_W$ using relativistic energy density functionals. The experimental data from PREX-II [15] and CREX [14] are denoted with vertical and horizontal bands.

and ΔR_{np} values obtained from the CREX experiment. As expected, the DDPC-CREX and DDPC-REX interactions fit into expected range of the $F_{ch} - F_W$ and ΔR_{np} values, since experimental value for F_W(^{48}Ca) is used in constraining their parameters. However, all other interactions that have previously been established as very successful in describing nuclear properties, e.g. DD-ME1, DD-ME2, DD-PC1, DD-PCX, remain above the experimental ranges for $F_{ch} - F_W$ and ΔR_{np} values. The only exception is DD-PC interaction with the $J = 29$ value. In this work, the neutron skin thickness values for ^{48}Ca are obtained as 0.218(5), 0.110(4), and 0.142(5) fm using the DDPC-PREX, DDPC-CREX, and DDPC-REX interactions, respectively. We note that in the present optimization of the EDFs, the weak-charge form factor data with small adopted errors are used in order to constrain the functionals that closely reproduce the experimental data on F_W, as previously introduced. Therefore, the symmetry energy and neutron-skin thickness values are both tightly constrained since these properties are strongly correlated with each other as well as with the weak-charge form factor data. Therefore, the obtained uncertainties in the neutron skin thickness values are small. It is seen that only the DDPC-REX result is in good agreement with the predictions of the *ab initio* theory ($0.12 \leq \Delta R_{np}^{48Ca} \leq 0.15$ fm) [35], and the recent results by including triples corrections in coupled-cluster theory ($0.13 \leq \Delta R_{np}^{48Ca} \leq 0.16$ fm) [36]. On the other hand, it is lower compared to the *model-averaged* values ($\Delta R_{np}^{48Ca} = 0.176 \pm 0.018$ fm) obtained in the EDF study in Ref. [9]. Using the linear fit obtained with different EDFs and the experimental limits for $F_{ch} - F_W$ values, the neutron skin

thickness is obtained between $0.098 \leq \Delta R_{np}^{48Ca} \leq 0.147$ fm, that is in better agreement with the *ab initio* theory predictions [35,36] than with the model-averaged EDF result [9].

As shown in Fig. 1, for ^{208}Pb, the experimental errors in $F_{ch} - F_W$ and ΔR_{np} obtained from PREX-II are larger, and more interactions fit into the experimental range of their values. However, all these interactions are on the opposite side of those preferred from the CREX experiment, in agreement with their larger values of the symmetry energy parameter J. Among new functionals, only DDPC-PREX fits into the experimental range of $F_{ch} - F_W$ and ΔR_{np} values, while DDPC-CREX and DDPC-REX results are obtained at considerably lower values. The DD-PCX and DD-ME2 functionals also remain below the experimental range, while DD-ME1 and DD-PC1 ones are very close to the lower experimental limits of $F_{ch} - F_W$ and ΔR_{np}. From the families of interactions that systematically vary the symmetry energy, only those with $J \geq 34$ (DD-ME) and $J \geq 34$ (DD-PC) are consistent with the PREX-II data. Employing DDPC-PREX, DDPC-CREX, and DDPC-REX functionals in the calculations, the neutron skin thickness values for ^{208}Pb are obtained as 0.250(10), 0.051(6), and 0.105(8) fm, respectively. The PREX-II measurements indicate a rather large neutron skin thickness value which is not in agreement neither with the *model-averaged* values ($\Delta R_{np}^{208Pb} = 0.168 \pm 0.0022$ fm) obtained in Ref. [9], nor with the limits obtained using the *ab initio* theory ($\Delta R_{np}^{208Pb} = 0.14 - 0.20$ fm) in Ref. [37]. Using the linear fit in Fig. 1 and experimental limits for $F_{ch} - F_W$ values, the neutron skin thickness is obtained between $0.202 \leq \Delta R_{np}^{208Pb} \leq 0.371$ fm for ^{208}Pb. Clearly, the limits are not in agreement with the previous model predictions [9,37].

The uncertainties in the model parameters and observables, and the correlations between them can be obtained with the statistical covariance analysis [38]. Within this framework, the coefficient of determination (CoD) is used to determine whether two observables have a genuine statistical correlation (CoD) or not. The CoD values range between 0 and 1. Two quantities are strongly correlated when CoD = 1, as opposed to being uncorrelated when CoD = 0. Additionally, the error ellipsoid between the two observables can be shown as the graphical representation of the CoD (see Refs. [38–40]). In Fig. 2, we display the error ellipsoids between ΔR_{np} and $F_{ch} - F_W$ for ^{48}Ca (upper panels) and ^{208}Pb (lower panels) using the new point-coupling functionals. The CoD numbers are also provided within the figures for each interaction and nucleus. Using three new point-coupling interactions, a strong correlation is obtained between the ΔR_{np} and $F_{ch} - F_W$ for both ^{48}Ca and ^{208}Pb. While the variances in the ellipsoids are slightly larger for ^{48}Ca in the perpendicular direction, the error ellipsoids are quite narrow for ^{208}Pb. Similar results are also obtained in Ref. [19] using the non-relativistic functionals.

Fig. 3 shows the summary of the neutron skin thicknesses values for ^{208}Pb obtained using DDPC-CREX, DDPC-PREX, and DDPC-REX functionals, in comparison to a number of previous experimental results [15,41–45]. In addition, the results of non-relativistic [46–48] and relativistic [20,21,34,47,49,50] studies based on the EDFs are shown, as well as the EDF constrained by chiral effective field theory, denoted as Skχm^* [48] (more details on other EDFs are given in the figure caption). One can observe that for ^{208}Pb the DDPC-CREX and DDPC-REX values for ΔR_{np} are smaller than those of all previous measurements and EDF predictions. On the other side, the DDPC-PREX functional provides ΔR_{np} value larger than obtained in most of the previous studies. It is in agreement with the PREX-II experiment, but also with the PC-PK1 interaction which has a higher value of the symmetry energy at saturation, $J = 35.6$ MeV. Clearly, the data from the parity-violating electron scattering experiments CREX and PREX-II could not provide a consistent understanding of the neutron
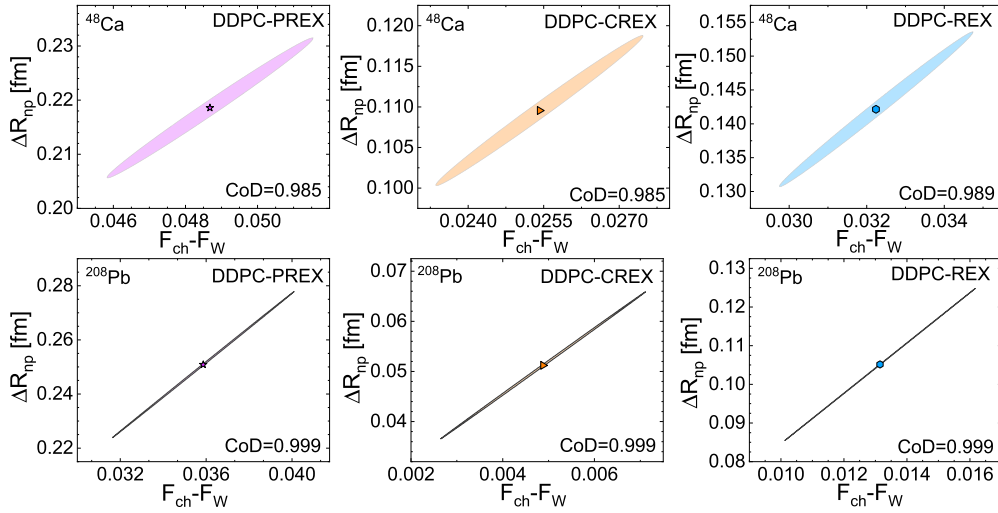
Fig. 2. The error ellipsoids between the neutron skin thickness ΔR_{np} and the form factor difference $F_{ch} - F_W$ for ^{48}Ca (upper panels) and ^{208}Pb (lower panels) using the new point-coupling interactions: DDPC-PREX, DDPC-CREX, and DDPC-REX. The CoD numbers are also given within the figures.
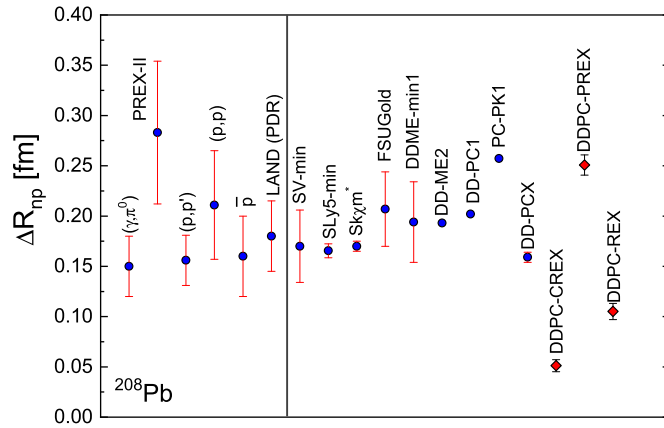

Fig. 3. The neutron skin thickness of ^{208}Pb for the DDPC-CREX, DDPC-PREX, and DDPC-REX functionals. For comparison, the experimental values are shown from (γ, π^0) [41], PREX-II [15], (p, p') [42], (p, p) [43], $\bar{p}$ [44], LAND (PDR) [45]. The results from the non-relativistic interactions include SV-min [46], SLy5-min [47], Skχm^* [48], and relativistic interactions: FSUGold [49], DDME-min1 [47], DD-ME2 [34], DD-PC1 [20], PC-PK1 [50], DD-PCX [21].

skin thickness in ^{208}Pb. Recent study of parity violating asymmetry A_{PV} in the EDF framework showed that simultaneous accurate description of A_{PV} in ^{48}Ca and ^{208}Pb could also not be achieved [19].

Another relevant quantity used in constraining the isovector channel of the EDFs is dipole polarizability α_D, corresponding to the sum of inverse energy weighted dipole transition strength in nuclei [7]. Over the past decade the dipole polarizability has attracted considerable interest because it is strongly correlated with the neutron form factor, neutron skin thickness [7,9–11], and the properties of the symmetry energy of nuclear matter [7]. Recently, the dipole polarizability has been measured for ^{48}Ca [51] and ^{208}Pb [42], and the corresponding values to be used in analyses are $\alpha_D(^{48}\text{Ca}) = 2.07 \pm 0.22$ fm^3 [51] and $\alpha_D(^{208}\text{Pb}) = 19.6 \pm 0.6$ fm^3 [11]. Therefore, it is interesting to confront the calculated values of α_D with those of $F_{ch} - F_W$, together with the corresponding experimental data, to assess the information which functional consistently describes these both quantities. The respective results are shown in Fig. 4, using the same density-dependent point coupling and meson exchange functionals as previously discussed. The horizontal and vertical bands denote the experimental values with errors for α_D and $F_{ch} - F_W$, respectively. As expected, strong cor-
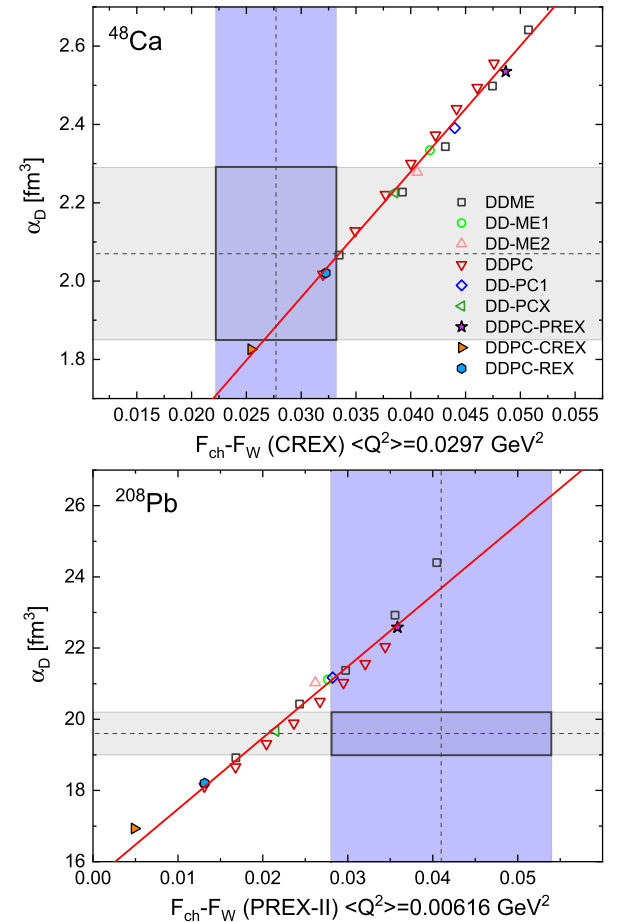

Fig. 4. The dipole polarizability α_D of ^{48}Ca (upper panel) and ^{208}Pb (lower panel) as a function of the form factor difference $F_{ch} - F_W$ using relativistic EDFs. Vertical bands denote $F_{ch} - F_W$ range of values from the CREX [14] and PREX-II [15] experiments, while horizontal bands correspond to the experimental data on α_D [11,42,51].

relation between α_D and $F_{ch} - F_W$ is obtained for ^{48}Ca and ^{208}Pb for all functionals used in the analysis. For ^{48}Ca, only one new interaction, DDPC-REX, and DDPC (J=29 MeV) are simultaneously within the experimental limits for α_D and $F_{ch} - F_W$ (CREX). The DDPC-CREX interaction gives a slightly smaller α_D value than the
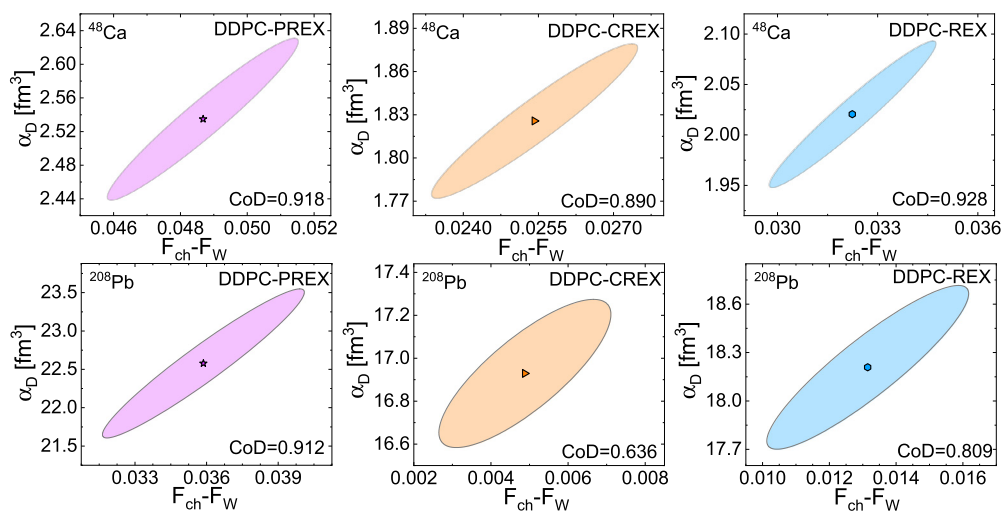
Fig. 5. The error ellipsoids between the dipole polarizability α_D and form factor difference $F_{ch} - F_W$ using new point coupling interactions for ^{48}Ca (upper panels) and ^{208}Pb (lower panels). The CoD values are also given within the figures.

lower experimental limit, while the DDPC-PREX interaction results for α_D and $F_{ch} - F_W$ are obtained at considerably higher values and above the experimental range. The DD-PCX interaction, which has been adjusted to reproduce experimental dipole polarizabilities, seems not consistent with $F_{ch} - F_W$ (CREX). For ^{48}Ca, the coupled cluster theory calculations predict $1.92 \leq \alpha_D(^{48}Ca) \leq 2.38$ fm^3, which is in agreement only with predictions of the DDPC-REX interaction [36].

Lower panel of Fig. 4, shows that for ^{208}Pb none of the new or previously established functionals can simultaneously reproduce experimental values for α_D and $F_{ch} - F_W$ (PREX-II). As expected, DDPC-PREX reproduces experimental form factors, but considerably overestimates α_D values. The DDPC-CREX and DDPC-REX underestimate both α_D and $F_{ch} - F_W$ (PREX-II) values. There is a considerable lack of consistency between the functionals constrained using CREX and PREX-II data when confronted with dipole polarizability studies. In Ref. [19], similar calculations have been performed using the non-relativistic functionals, and a strong correlation is also obtained between the parity violating asymmetry A_{PV} and $J\alpha_D$. Since A_{PV} is directly correlated with the F_{ch} and F_W, our findings are consistent.

Fig. 5 shows the error ellipsoids between the α_D and $F_{ch} - F_W$ for the new point-coupling interactions. The results are displayed for ^{48}Ca (upper panels) and ^{208}Pb (lower panels). For both nuclei, there is a strong correlation between α_D and $F_{ch} - F_W$ using three functionals, albeit smaller when compared to ΔR_{np} and $F_{ch} - F_W$. The lowest CoD value between the α_D and $F_{ch} - F_W$ is obtained for ^{208}Pb using the DDPC-CREX functional.

In summary, the weak-charge form factors from parity-violating electron scattering open an important new perspective to constrain the neutron skins and the properties of the nuclear matter symmetry energy. In this work, the weak-charge form factors obtained from the CREX and PREX-II data have been used directly in constraining the relativistic EDFs, having in this way a considerable impact on their isovector interaction channel. However, the neutron skin thicknesses calculated from these EDFs do not seem consistent, and they are at variance with respect to previous theoretical and experimental studies. When the weak-charge form factors are confronted with the dipole polarizability, the results of the analysis show significant inconsistencies, although both should probe the same content of the EDFs. The symmetry energy and its slope at saturation density, as well as the neutron skin thickness, are significantly smaller for the DDPC-CREX functional in comparison to those of the DDPC-PREX, and values established by previous

EDFs are between those obtained with the two new functionals. The analysis of this work shows that no consistent conclusions from the theoretical side could be obtained when using recent CREX and PREX-II results. Clearly, further EDF and *ab-initio* studies, alongside with novel experimental investigations are needed to resolve the current puzzling implications of the parity violating electron scattering data.

Declaration of competing interest

The authors declare that they have no known competing financial interests or personal relationships that could have appeared to influence the work reported in this paper.

Data availability

Data will be made available on request.

Acknowledgements

Appendix A. Supplementary material

Supplementary material related to this article can be found online at https://doi.org/10.1016/j.physletb.2022.137622.

References

[1] J.M. Lattimer, Annu. Rev. Nucl. Part. Sci. 62 (2012) 485, https://doi.org/10.1146/annurev-nucl-102711-095018.
[2] M. Oertel, M. Hempel, T. Klähn, S. Typel, Rev. Mod. Phys. 89 (2017) 015007.
[3] X. Roca-Maza, N. Paar, Prog. Part. Nucl. Phys. 101 (2018) 96.
[4] B. Alex Brown, Phys. Rev. Lett. 85 (2000) 5296.
[5] M.B. Tsang, J.R. Stone, F. Camera, P. Danielewicz, S. Gandolfi, K. Hebeler, C.J. Horowitz, J. Lee, W.G. Lynch, Z. Kohley, R. Lemmon, P. Möller, T. Murakami, S. Riordan, X. Roca-Maza, F. Sammarruca, A.W. Steiner, I. Vidaña, S.J. Yennello, Phys. Rev. C 86 (2012) 015803.
[6] A. Tamii, P. von Neumann-Cosel, I. Poltoratska, Eur. Phys. J. A 50 (2014), https://doi.org/10.1140/epja/i2014-14028-7.
[7] P.-G. Reinhard, W. Nazarewicz, Phys. Rev. C 81 (2010) 051303.
[8] S. Typel, B.A. Brown, Phys. Rev. C 64 (2001) 027302.

[9] J. Piekarewicz, B.K. Agrawal, G. Colò, W. Nazarewicz, N. Paar, P.-G. Reinhard, X. Roca-Maza, D. Vretenar, Phys. Rev. C 85 (2012) 041302.

[10] X. Roca-Maza, M. Brenna, G. Colò, M. Centelles, X. Viñas, B.K. Agrawal, N. Paar, D. Vretenar, J. Piekarewicz, Phys. Rev. C 88 (2013) 024316.

[11] X. Roca-Maza, X. Viñas, M. Centelles, B.K. Agrawal, G. Colò, N. Paar, J. Piekarewicz, D. Vretenar, Phys. Rev. C 92 (2015) 064304.

[12] J.M. Lattimer, A.W. Steiner, Eur. Phys. J. A 50 (2014), https://doi.org/10.1140/epja/i2014-14040-y.

[13] G. Burgio, H.-J. Schulze, I. Vidaña, J.-B. Wei, Prog. Part. Nucl. Phys. 120 (2021) 103879.

[14] D. Adhikari, H. Albataineh, D. Androic, K.A. Aniol, D.S. Armstrong, T. Averett, C. Ayerbe Gayoso, S.K. Barcus, V. Bellini, R.S. Beminiwattha, J.F. Benesch, H. Bhatt, D. Bhatta Pathak, D. Bhetuwal, B. Blaikie, J. Boyd, Q. Campagna, A. Camsonne, G.D. Cates, Y. Chen, C. Clarke, J.C. Cornejo, S. Covrig Dusa, M.M. Dalton, P. Datta, A. Deshpande, D. Dutta, C. Feldman, E. Fuchey, C. Gal, D. Gaskell, T. Gautam, M. Gericke, C. Ghosh, I. Halilovic, J.-O. Hansen, O. Hassan, F. Hauenstein, W. Henry, C.J. Horowitz, C. Jantzi, S. Jian, S. Johnston, D.C. Jones, S. Kakkar, S. Katugampola, C. Keppel, P.M. King, D.E. King, K.S. Kumar, T. Kutz, N. Lashley-Colthirst, G. Leverick, H. Liu, N. Liyanage, J. Mammei, R. Mammei, M. McCaughan, D. McNulty, D. Meekins, C. Metts, R. Michaels, M. Mihovilovic, M.M. Mondal, J. Napolitano, A. Narayan, D. Nikolaev, V. Owen, C. Palatchi, J. Pan, B. Pandey, S. Park, K.D. Paschke, M. Petrusky, M.L. Pitt, S. Premathilake, B. Quinn, R. Radloff, S. Rahman, M.N.H. Rashad, A. Rathnayake, B.T. Reed, P.E. Reimer, R. Richards, S. Riordan, Y.R. Roblin, S. Seeds, A. Shahinyan, P. Souder, M. Thiel, Y. Tian, G.M. Urciuoli, E.W. Wertz, B. Wojtsekhowski, B. Yale, T. Ye, A. Yoon, W. Xiong, A. Zec, W. Zhang, J. Zhang, X. Zheng, PREX Collaboration, Phys. Rev. Lett. 129 (2022) 042501.

[15] D. Adhikari, H. Albataineh, D. Androic, K. Aniol, D.S. Armstrong, T. Averett, C. Ayerbe Gayoso, S. Barcus, V. Bellini, R.S. Beminiwattha, J.F. Benesch, H. Bhatt, D. Bhatta Pathak, D. Bhetuwal, B. Blaikie, Q. Campagna, A. Camsonne, G.D. Cates, Y. Chen, C. Clarke, J.C. Cornejo, S. Covrig Dusa, P. Datta, A. Deshpande, D. Dutta, C. Feldman, E. Fuchey, C. Gal, D. Gaskell, T. Gautam, M. Gericke, C. Ghosh, I. Halilovic, J.-O. Hansen, F. Hauenstein, W. Henry, C.J. Horowitz, C. Jantzi, S. Jian, S. Johnston, D.C. Jones, B. Karki, S. Katugampola, C. Keppel, P.M. King, D.E. King, M. Knauss, K.S. Kumar, T. Kutz, N. Lashley-Colthirst, G. Leverick, H. Liu, N. Liyanage, S. Malace, R. Mammei, J. Mammei, M. McCaughan, D. McNulty, D. Meekins, C. Metts, R. Michaels, M.M. Mondal, J. Napolitano, A. Narayan, D. Nikolaev, M.N.H. Rashad, V. Owen, C. Palatchi, J. Pan, B. Pandey, S. Park, K.D. Paschke, M. Petrusky, M.L. Pitt, S. Premathilake, A.J.R. Puckett, B. Quinn, R. Radloff, S. Rahman, A. Rathnayake, B.T. Reed, P.E. Reimer, R. Richards, S. Riordan, Y. Roblin, S. Seeds, A. Shahinyan, P. Souder, L. Tang, M. Thiel, Y. Tian, G.M. Urciuoli, E.W. Wertz, B. Wojtsekhowski, B. Yale, T. Ye, A. Yoon, A. Zec, W. Zhang, J. Zhang, X. Zheng, PREX Collaboration, Phys. Rev. Lett. 126 (2021) 172502.

[16] P.-G. Reinhard, J. Piekarewicz, W. Nazarewicz, B.K. Agrawal, N. Paar, X. Roca-Maza, Phys. Rev. C 88 (2013) 034325.

[17] C.J. Horowitz, S.J. Pollock, P.A. Souder, R. Michaels, Phys. Rev. C 63 (2001) 025501.

[18] P.-G. Reinhard, X. Roca-Maza, W. Nazarewicz, Phys. Rev. Lett. 127 (2021) 232501.

[19] P.-G. Reinhard, X. Roca-Maza, W. Nazarewicz, Phys. Rev. Lett. 129 (2022) 232501.

[20] T. Nikšić, D. Vretenar, P. Ring, Phys. Rev. C 78 (2008) 034318.

[21] E. Yüksel, T. Marketin, N. Paar, Phys. Rev. C 99 (2019) 034318.

[22] W. Kohn, L.J. Sham, Phys. Rev. 140 (1965) A1133.

[23] W. Kohn, Rev. Mod. Phys. 71 (1999) 1253.

[24] T. Nikšić, N. Paar, D. Vretenar, P. Ring, Comput. Phys. Commun. 185 (2014) 1808.

[25] D. Vretenar, A. Afanasjev, G. Lalazissis, P. Ring, Phys. Rep. 409 (2005) 101.

[26] Y. Tian, Z.-y. Ma, P. Ring, Phys. Rev. C 80 (2009) 024313.

[27] X. Roca-Maza, N. Paar, G. Colò, J. Phys. G, Nucl. Part. Phys. 42 (2015) 034033.

[28] E. Yüksel, N. Paar, See Supplemental Material at https://doi.org/10.1016/j.physletb.2022.137622 for the new interaction paramaters.

[29] J. Dobaczewski, W. Nazarewicz, P.-G. Reinhard, J. Phys. G, Nucl. Part. Phys. 41 (2014) 074001.

[30] B.T. Reed, F.J. Fattoyev, C.J. Horowitz, J. Piekarewicz, Phys. Rev. Lett. 126 (2021) 172503.

[31] S. Abrahamyan, Z. Ahmed, H. Albataineh, K. Aniol, D.S. Armstrong, W. Armstrong, T. Averett, B. Babineau, A. Barbieri, V. Bellini, R. Beminiwattha, J. Benesch, F. Benmokhtar, T. Bielarski, W. Boeglin, A. Camsonne, M. Canan, P. Carter, G.D. Cates, C. Chen, J.-P. Chen, O. Hen, F. Cusanno, M.M. Dalton, R. De Leo, K. de Jager, W. Deconinck, P. Decowski, X. Deng, A. Deur, D. Dutta, A. Etile,

D. Flay, G.B. Franklin, M. Friend, S. Frullani, E. Fuchey, F. Garibaldi, E. Gasser, R. Gilman, A. Giusa, A. Glamazdin, J. Gomez, J. Grames, C. Gu, O. Hansen, J. Hansknecht, D.W. Higinbotham, R.S. Holmes, T. Holmstrom, C.J. Horowitz, J. Hoskins, J. Huang, C.E. Hyde, F. Itard, C.-M. Jen, E. Jensen, G. Jin, S. Johnston, A. Kelleher, K. Kliakhandler, P.M. King, S. Kowalski, K.S. Kumar, J. Leacock, J. Leckey, J.H. Lee, J.J. LeRose, R. Lindgren, N. Liyanage, N. Lubinsky, J. Mammei, F. Mammoliti, D.J. Margaziotis, P. Markowitz, A. McCreary, D. McNulty, L. Mercado, Z.-E. Meziani, R.W. Michaels, M. Mihovilovic, N. Muangma, C. Muñoz Camacho, S. Nanda, V. Nelyubin, N. Nuruzzaman, Y. Oh, A. Palmer, D. Parno, K.D. Paschke, S.K. Phillips, B. Poelker, R. Pomatsalyuk, M. Posik, A.J.R. Puckett, B. Quinn, A. Rakhman, P.E. Reimer, S. Riordan, P. Rogan, G. Ron, G. Russo, K. Saenboonruang, A. Saha, B. Sawatzky, A. Shahinyan, R. Silwal, S. Sirca, K. Slifer, P. Solvignon, P.A. Souder, M.L. Sperduto, R. Subedi, R. Suleiman, V. Sulkosky, C.M. Sutera, W.A. Tobias, W. Troth, G.M. Urciuoli, B. Waidyawansa, D. Wang, J. Wexler, R. Wilson, B. Wojtsekhowski, X. Yan, H. Yao, Y. Ye, Z. Ye, V. Yim, L. Zana, X. Zhan, J. Zhang, Y. Zhang, X. Zheng, P. Zhu, PREX Collaboration, Phys. Rev. Lett. 108 (2012) 112502.

[32] E. Yüksel, T. Oishi, N. Paar, Universe 7 (2021), https://doi.org/10.3390/universe7030071.

[33] T. Nikšić, D. Vretenar, P. Finelli, P. Ring, Phys. Rev. C 66 (2002) 024306.

[34] G.A. Lalazissis, T. Nikšić, D. Vretenar, P. Ring, Phys. Rev. C 71 (2005) 024312.

[35] G. Hagen, A. Ekström, C. Forssén, G.R. Jansen, W. Nazarewicz, T. Papenbrock, K.A. Wendt, S. Bacca, N. Barnea, B. Carlsson, C. Drischler, K. Hebeler, M. Hjorth-Jensen, M. Miorelli, G. Orlandini, A. Schwenk, J. Simonis, Nat. Phys. 12 (2016) 186.

[36] J. Simonis, S. Bacca, G. Hagen, Eur. Phys. J. A 55 (2019) 241.

[37] B. Hu, W. Jiang, T. Miyagi, Z. Sun, A. Ekström, C. Forssén, G. Hagen, J.D. Holt, T. Papenbrock, S.R. Stroberg, I. Vernon, https://doi.org/10.48550/ARXIV.2112.01125, 2021.

[38] J. Dobaczewski, W. Nazarewicz, P.-G. Reinhard, J. Phys. G, Nucl. Part. Phys. 41 (2014) 074001.

[39] J. Erler, P.-G. Reinhard, J. Phys. G, Nucl. Part. Phys. 42 (2015) 034026.

[40] P.-G. Reinhard, Phys. Scr. 91 (2016) 023002.

[41] C.M. Tarbert, D.P. Watts, D.I. Glazier, P. Aguar, J. Ahrens, J.R.M. Annand, H.J. Arends, R. Beck, V. Bekrenev, B. Boillat, A. Braghieri, D. Branford, W.J. Briscoe, J. Brudvik, S. Cherepnya, R. Codling, E.J. Downie, K. Foehl, P. Grabmayr, R. Gregor, E. Heid, D. Hornidge, O. Jahn, V.L. Kashevarov, A. Knezevic, R. Kondratiev, M. Korolija, M. Kotulla, D. Krambrich, B. Krusche, M. Lang, V. Lisin, K. Livingston, S. Lugert, I.J.D. MacGregor, D.M. Manley, M. Martinez, J.C. McGeorge, D. Mekterovic, V. Metag, B.M.K. Nefkens, A. Nikolaev, R. Novotny, R.O. Owens, P. Pedroni, A. Polonski, S.N. Prakhov, J.W. Price, G. Rosner, M. Rost, T. Rostomyan, S. Schadmand, S. Schumann, D. Sober, A. Starostin, I. Supek, A. Thomas, M. Unverzagt, T. Walcher, L. Zana, F. Zehr, Crystal Ball at MAMI and A2 Collaboration, Phys. Rev. Lett. 112 (2014) 242502.

[42] A. Tamii, I. Poltoratska, P. von Neumann-Cosel, Y. Fujita, T. Adachi, C.A. Bertulani, J. Carter, M. Dozono, H. Fujita, K. Fujita, K. Hatanaka, D. Ishikawa, M. Itoh, T. Kawabata, Y. Kalmykov, A.M. Krumbholz, E. Litvinova, H. Matsubara, K. Nakanishi, R. Neveling, H. Okamura, H.J. Ong, B. Özel-Tashenov, V.Y. Ponomarev, A. Richter, B. Rubio, H. Sakaguchi, Y. Sakemi, Y. Sasamoto, Y. Shimbara, Y. Shimizu, F.D. Smit, T. Suzuki, Y. Tameshige, J. Wambach, R. Yamada, M. Yosoi, J. Zenihiro, Phys. Rev. Lett. 107 (2011) 062502.

[43] J. Zenihiro, H. Sakaguchi, T. Murakami, M. Yosoi, Y. Yasuda, S. Terashima, Y. Iwao, H. Takeda, M. Itoh, H.P. Yoshida, M. Uchida, Phys. Rev. C 82 (2010) 044611.

[44] A. Kłos, A. Trzcińska, J. Jastrzębski, T. Czosnyka, M. Kisieliński, P. Lubiński, P. Napiorkowski, L. Pieńkowski, F.J. Hartmann, B. Ketzer, P. Ring, R. Schmidt, T. v. Egidy, R. Smolańczuk, S. Wycech, K. Gulda, W. Kurcewicz, E. Widmann, B.A. Brown, Phys. Rev. C 76 (2007) 014311.

[45] A. Klimkiewicz, N. Paar, P. Adrich, M. Fallot, K. Boretzky, T. Aumann, D. Cortina-Gil, U.D. Pramanik, T.W. Elze, H. Emling, H. Geissel, M. Hellström, K.L. Jones, J.V. Kratz, R. Kulessa, C. Nociforo, R. Palit, H. Simon, G. Surówka, K. Sümmerer, D. Vretenar, W. Waluś, LAND Collaboration, Phys. Rev. C 76 (2007) 051603.

[46] P. Klüpfel, P.-G. Reinhard, T.J. Bürvenich, J.A. Maruhn, Phys. Rev. C 79 (2009) 034310.

[47] X. Roca-Maza, N. Paar, G. Colò, J. Phys. G, Nucl. Part. Phys. 42 (2015) 034033.

[48] Z. Zhang, Y. Lim, J.W. Holt, C.M. Ko, Phys. Lett. B 777 (2018) 73.

[49] B.G. Todd-Rutel, J. Piekarewicz, Phys. Rev. Lett. 95 (2005) 122501.

[50] P.W. Zhao, Z.P. Li, J.M. Yao, J. Meng, Phys. Rev. C 82 (2010) 054319.

[51] J. Birkhan, M. Miorelli, S. Bacca, S. Bassauer, C.A. Bertulani, G. Hagen, H. Matsubara, P. von Neumann-Cosel, T. Papenbrock, N. Pietralla, V.Y. Ponomarev, A. Richter, A. Schwenk, A. Tamii, Phys. Rev. Lett. 118 (2017) 252501.